

PAPER • OPEN ACCESS

## Structural and dynamic assessment of a friction buffer stop

To cite this article: G Megna and A Bracciali 2024 *IOP Conf. Ser.: Mater. Sci. Eng.* **1306** 012022

View the [article online](#) for updates and enhancements.

You may also like

- [Phylogenetic analysis of Gayo and Toraya buffalo breed of Indonesian through mitochondrial D-loop region](#)  
E M Sari, M A N Abdullah, H Koesmara et al.
- [Buffer Pka Impacts the Mechanism of Hydrogen Evolution in Water Catalyzed By a Cobalt Porphyrin-Peptide](#)  
Jose L. Alvarez-Hernandez, Andrew Sopchak and Kara Bren
- [The role of grazing land on the buffalo population dynamics in Brebes regency](#)  
Sumanto



The Electrochemical Society  
Advancing solid state & electrochemical science & technology

**DISCOVER**  
how sustainability  
intersects with  
electrochemistry & solid  
state science research



# Structural and dynamic assessment of a friction buffer stop

**G Megna, A Bracciali**

Department of Industrial Engineering (DIEF), Università degli studi di Firenze, Via S. Marta 3, 50139, Firenze

gianluca.megna@unifi.it

**Abstract.** Under peculiar conditions railway braking system can fail giving insufficient braking force during train ride or while standstill and buffer stops are used to avoid derailments at the end of railway tracks (dead tracks). Fixed stops are suitable only for quasi-static movements, while absorbing energy stops using hydraulic cylinders, friction shoes clamped on the rail head or a combination of both methods, are installed if crashes at higher speeds (about 25 km/h) are forecasted. Impact forces generated due to the interaction between train and buffer stops require a suitable design of the steel structure which is subjected to stress values depending on the braking performances of the buffer stop itself and a combined structural and dynamic analysis must be carried out to perform a proper design. Due to unavailability of detailed models and the uncertainties of the actual braking performances, the structure of currently available friction buffer stops is heavy and bulky, made of several steel profiles welded or bolted to each other. The paper describes an innovative and optimized design for friction buffer stops focusing on the dynamic analysis performed by Finite Element Method to assess the braking performances and structural strength of the buffer stop.

## 1. Introduction

As the braking system is designed with the aim to reduce passenger discomfort (low deceleration values) and to avoid wheel slip in almost all wheel-rail contact conditions, railway vehicles are characterized by high stopping distances. The braking force is evaluated considering a maximum available adhesion of  $f=0.15$  [1] and anti-slip systems are installed on board to modulate the braking force in case of low adhesion conditions.

However, in certain situations, as for the “leaves on the line” case, which is a common issue in autumn especially in Great Britain, wheel slip cannot be avoided, furtherly increasing the stopping distances [2]. In other cases, trains can move from standstill position, especially if very long-time stops are planned, due to brake failure and insufficient immobilization given by handbrake or shoes placed under the wheels.

Braking failures must be carefully evaluated and mitigated as they are directly related to safety involving collisions due to SPADs (Signals Passed At Danger), station overruns and derailments at dead end tracks and low adhesion conditions are still deeply studied [3-5]. To avoid derailments at the end of the tracks, an increasing number of buffer stops is installed on railway lines.



Buffer stops can be fixed, which are directly bolted to the rails and can withstand only quasi-static movements, or with absorbing energy systems if crashes at higher speed must be mitigated. Hydraulic cylinders, friction shoes clamped to the rails or a combination of both are the common methods used for this kind of buffer stops (see figure 1).

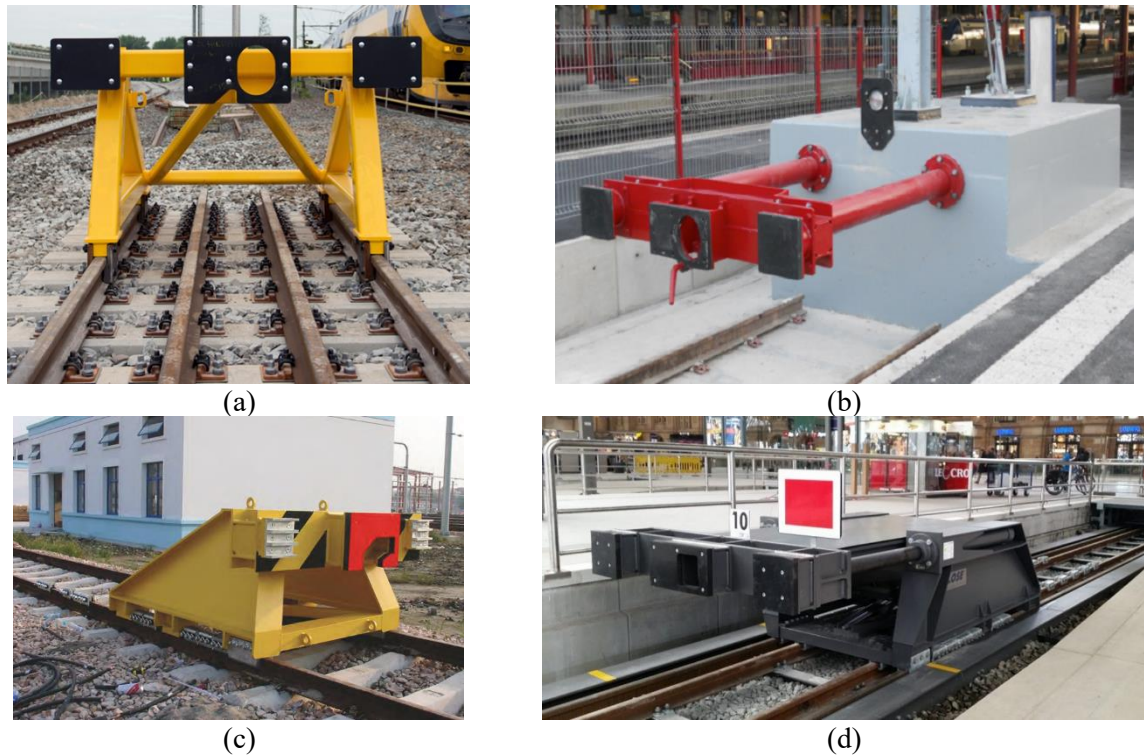


**Figure 1.** Example of buffer stops with different configurations: a) fixed; (b) hydraulic; (c) friction; (d) hydraulic and friction.

The choice of the buffer stop depends on the design requirements in terms of vehicle mass  $m$  and speed  $v$ , resulting in the total kinetic energy to be dissipated according to equation (1).

$$E = \frac{1}{2}mv^2 \quad (1)$$

Depending on the combination of mass and speed the maximum energy to be dissipated is defined. For example, the Italian requirements for friction buffer stops [6] are described in table 1. In both cases the maximum deceleration rate is fixed at  $2 \text{ m/s}^2$ . Different specifications exist in other countries, especially for vehicle mass which can reach up to  $3500 \text{ t}$  [7], but in the following only the Italian standard is considered.

**Table 1.** Requirements of friction buffers stops according to Italian standard [6]

Load case	Mass [t]	Speed [km/h]	Energy [kJ]	Stopping distance [m]
1	650	15	5700	10
2	500	10	2000	5

About structural strength, buffer stops must be designed to survive for at least 40 years with one major impact (load case 1) and six medium impacts (load case 2) per year.

## 2. Design and limitations of existing friction buffer stops

Two main drawbacks are present in the current design of friction buffer stops:

- braking blocks (clamps) are made of several components and are clamped to rail head with several uncertainties about mounting position and preload conditions;
- reinforcing elements are needed to limit track lifting and rail stress in case of major impacts.

These issues increase the complexity of the buffer stop installation and the uncertainty of its dynamic performances, which are estimated by simple analytical models in which the braking forces exerted by the clamps are based on simplified assumptions.

A typical clamp is shown in figure 2(a). Friction forces are generated by the sliding of a cast iron block on the rail head while the preload is provided by two bent steel fishplates fastened by three M24 bolts. Two brass sliding chairs complete the assembly on the lower faces of the rail head. The mounting position is not unique as it suffers from uncertainties due to tolerances as shown in figure 2(b), and a proper calculation of the preload force and therefore of the friction force is not possible. Phosphoric P10 cast iron, i.e. the same material used on vehicles braking shoes [8] is used.

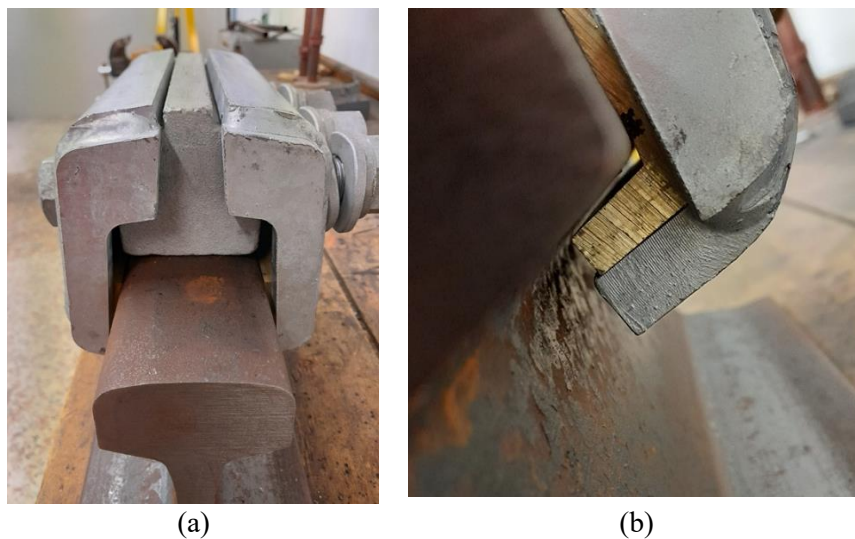


**Figure 2.** Existing braking element (clamp) for friction buffer stop (a) and detail of its mounting position on the rail head (b).

The large amount of energy to be dissipated results in high impact forces and due to the height difference between the impact force and the braking blocks, about 1000 mm, an upward vertical force on the back of the buffer stop is generated. This force is such that the rails are raised, as the track in its common configuration, i.e. ballasted track, does not provide any resistance to upward movements. A prediction of the vertical displacement of the rail and therefore the generated stress is not easy to perform without the use of realistic models including the complete buffer stop and its interaction with the track.

Therefore, in the current design a reinforcing system of the track is required for major impacts, as shown in figure 3. The stiffening of the track consists in placing below the rail other steel beams, or another rail, connected to the main one by special connections. The buffer stop construction and installation costs are therefore noticeably increased. The simplified analytical models used to calculate the stress on the rails do not consider the dynamic effects of the impact and the actual contribution of

the track components, such as the sleepers inertia, and the reaction forces ahead and back to the buffer stop. The reaction force ahead is given by the buffer stop itself, while the reaction force on the back is given by the vertical wheel load of the impacting vehicle. The design of buffer stops for load case 1 and for load case 2 is completely different, with resulting higher costs.

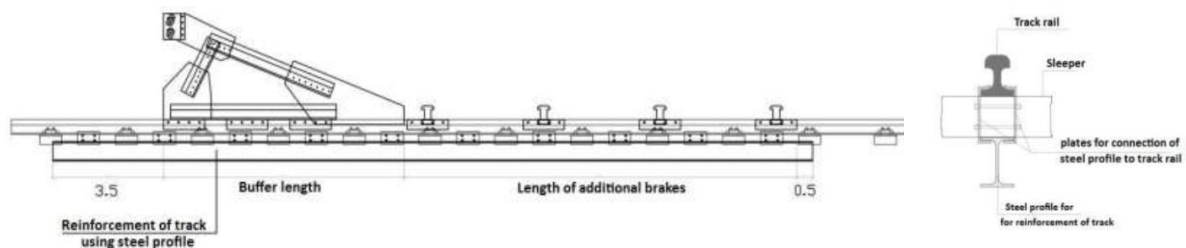


**Figure 3.** Example of track reinforcement [7]

The aim of this work is to design a new buffer stop with a simplified structure capable to satisfy all the requirements of the Italian standard [6] with a single configuration that does not require track reinforcements. For this scope a detailed model of the buffer stop and the track was developed including the actual friction behaviour of the clamps that were modified to reduce the number of components and to simplify the preload calculation.

### 3. Modelling and analysis of the new friction buffer stop

#### 3.1. Description of the new buffer stop structure

The new buffer stop is shown in figure 4. Its innovative configuration consists in a main beam *a*) with the interfaces for the interaction with either the vehicle's buffers [9] or the central automatic coupling device [10]. The impact force is transferred from the buffer stop structure to the rail, where the clamps *c*) are fastened, by means of a strut made of a tubular steel beam *b*).

The moment generated by the height difference is balanced by a vertical force passing through the rod *d*), which is responsible for the vertical upward movement of the rail. This force is split in two identical components acting at 2 m distance to each other by a triangular structure *e*) made of two steel sheets clamped without preload to the rail head. All the components are connected by cylindrical joints, and the mechanism is closed by two rods *f*) connecting the front and the rear of the buffer stop. The structure is completed by two crossing steel ropes *g*) connecting the two sides of the buffer stop to cope with any possible asymmetric braking conditions.

The clamp is designed with only two cast iron components, connected by two M16 bolts, with a rail-like shape to generate a pressure on the rail head surface when the bolts are preloaded. The forces acting on the clamp during the preloading phase are shown in figure 5(a) while the corresponding deformation is shown in figure 5(b). The preload is calculated considering a frictionless phase while the load of the bolts is applied, reaching the maximum value at the end the load application. The pressure values reached at the end of the preload application are shown in Figure 5(c). A friction coefficient of 0.2 is considered to reproduce the dynamic interaction between the cast iron clamp and the steel rail head, reaching a braking force of about 90 kN, which is nearly double than the one in the current configurations.

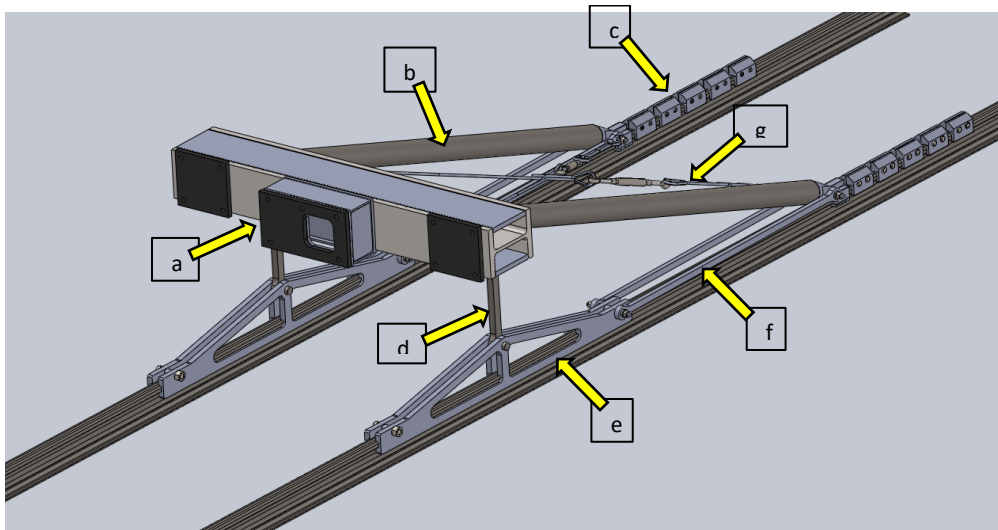
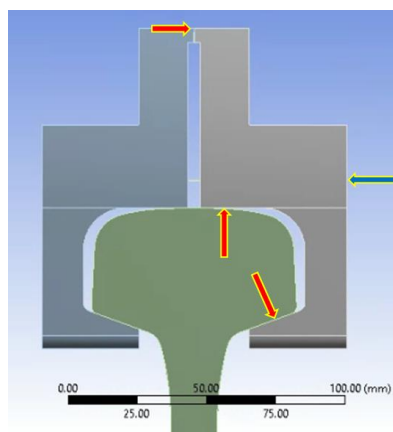
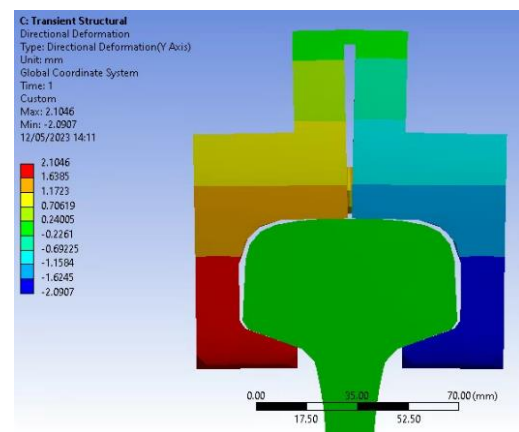


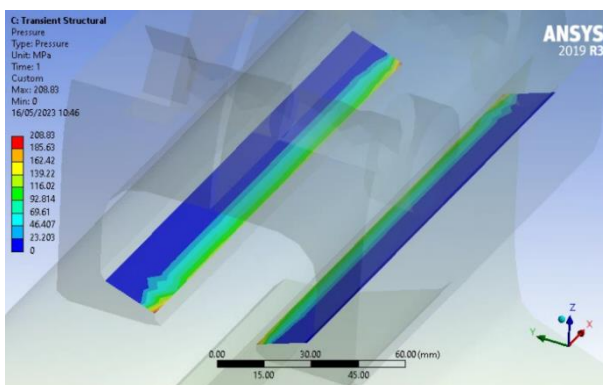
**Figure 4.** Description of the structure of the new friction buffer stop



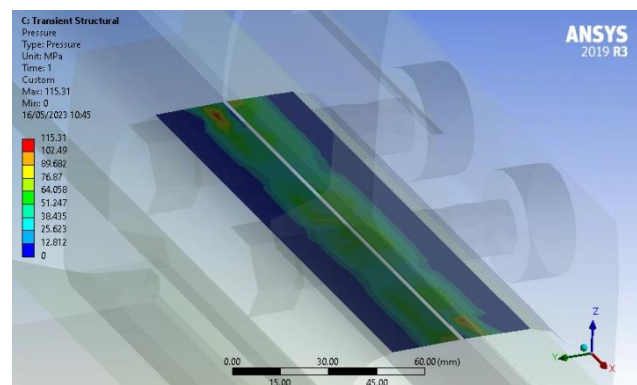
(a)



(b)



(c)



(d)

**Figure 5.** Forces acting on the clamp during the preloading phase (a). Displacements of the two cast iron blocks after the preload application to the bolts (b). Pressure map at the bottom faces of the rail head (c) Pressure map at the top of the rail head (d).

### 3.2. Dynamic model description

A strongly nonlinear dynamic model of the buffer stop was developed to simulate the complete interaction between the buffer stop and the track during the transient phases of the impact until a complete stop.

A general view of the model is shown in figure 6(a), which represent a 24 m long track section including 18 m of rail modelled with solid elements. When symmetric braking conditions are analysed only half model is considered to reduce the computational time. Sleepers are represented by point masses of 150 kg attached to the rail, while the vertical support of the rail is made of non-linear connections with  $k_z=0$  for upward movements (free) and  $k_z=100$  kN/mm for downward movements (reacted by the ballast).

Upward movements of the track are limited by inertial forces, by the elastic properties of the rail and by a downward vertical force due to the axleload of the first wheel of the vehicle hitting the buffer stop. The latter moves together with the buffer stop, locking their longitudinal connection at the impact to keep their distance constant (3 m). This kind of modelling allows to find the actual deformation of the track during the impact, evaluating the need of reinforcements if its strength is not sufficient. The rail is free to move longitudinally at the end of the track, while the lateral displacements and the longitudinal (about  $x$  axis) and vertical (about  $z$  axis) rotations are constrained at the sleeper positions (sleeper span = 600 mm).

The impact is simulated with two solids (one with zero mass simulating the vehicle buffer plate and one including the whole hitting mass) longitudinally connected by a flexible element representing the elastic behavior of the vehicle buffer when compressed. The non-linear stiffness of the vehicle buffer according to [9] was simplified with a bilinear curve for a maximum deformation of 100 mm, as shown in figure 6(b) and (c). The position of the masses, which is fixed during the whole simulation, is given by  $y=1750/2=875$  mm and  $z=1050$  mm. The contact between the first mass and the buffer stop beam was modelled as a frictionless contact with all the degrees of freedom free, except for the longitudinal displacement which is locked in the moment of the impact. Although, this simulates an inelastic collision between the impact masses and the buffer stop, the vehicle buffer mass is negligible compared to the hitting masses with no consequences on the total kinetic energy.

The distance between the masses and the buffer stop is 500 mm and the simulation is divided in two steps: in the first step the masses cover the 500 mm distance and at the same time the bolt preloads are applied to the clamps, while in the second step the impact occurs, and the braking force is applied by the frictional contacts between the clamps and the rail. The initial distance between clamps is 50 mm and they are pushed with frictionless contacts between their front and rear surfaces. The first clamp connected to the strut by a hinge is not preloaded, but it generates the vertical components of the reaction force and a frictional contact between the clamp and the rail head is also modelled contributing to the total braking force.

The vertical reaction force is balanced by the rod below the main beam which is connected to the triangular structure that splits the force by contact surfaces at the bottom faces of the rails. Friction is exerted also on these surfaces with a friction coefficient of 0.1 due to the absence of preload. The vertical rod is connected by hinges to the strut at its top and to the triangular structure at its bottom. The mechanism is completed by two rods connecting the front and the rear part of the buffer stop.

A complete model was developed to check the buffer stop behavior and the cross-bracing connections in case of asymmetric braking forces, as shown in figure 7 in which one clamp preload was removed on one side of the buffer stop.

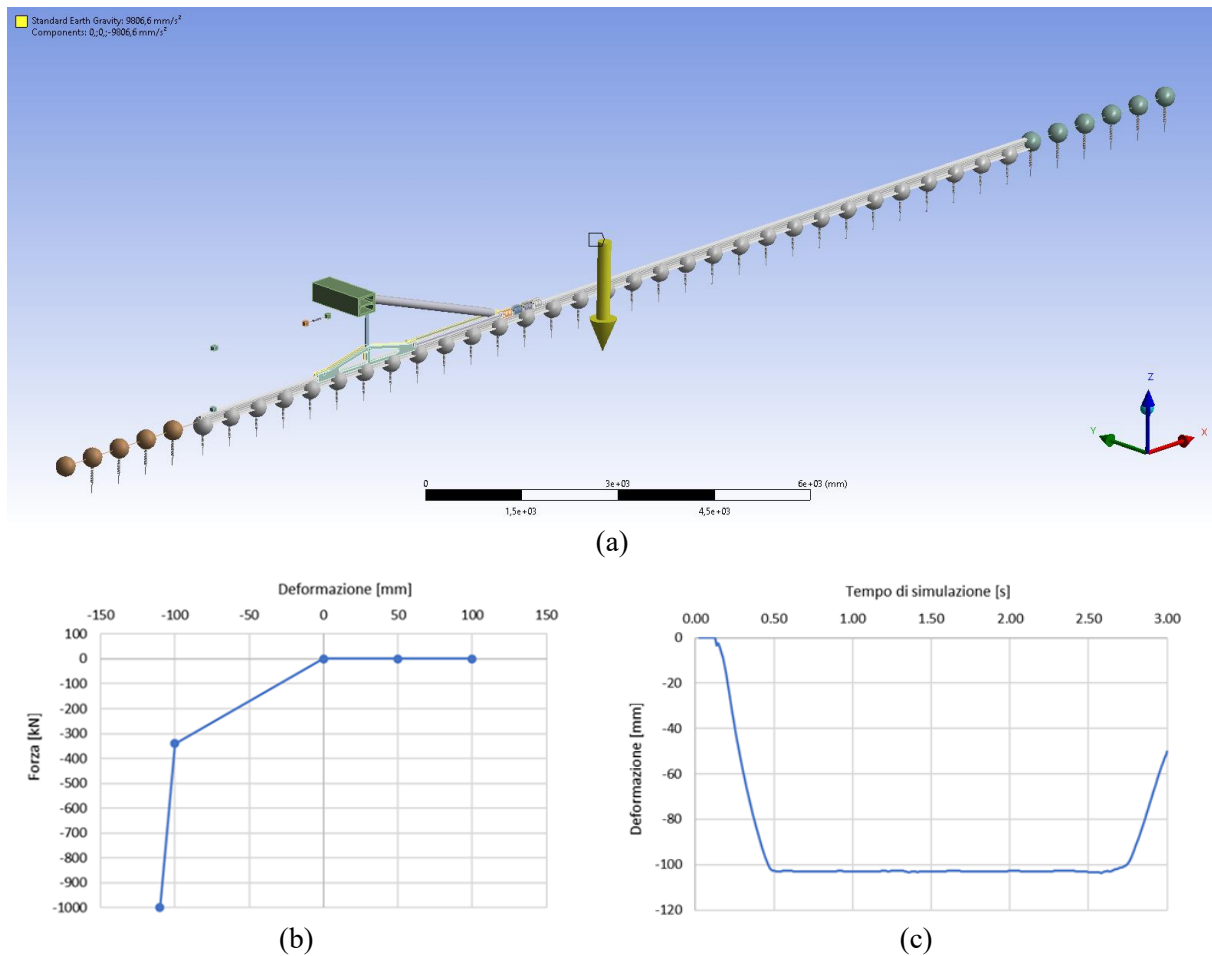


**Figure 6.** General view of the dynamic model (a). Force-displacement curve of the elastic element between the impact masses (b). Longitudinal deformation of the elastic element during a simulation.

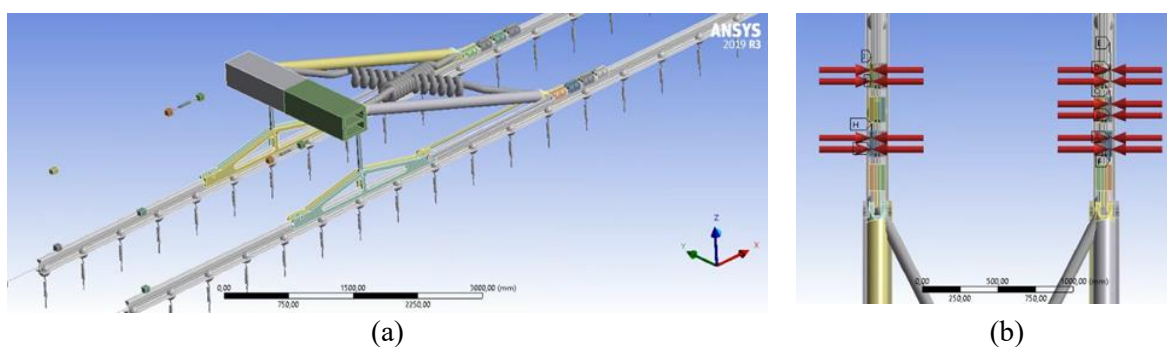


**Figure 7.** Complete buffer stop model including the crossing connections (a). Asymmetric braking conditions due missing preload on one side (b).

### 3.3. Results of the dynamic analyses

Several analyses were performed varying the impact mass and the speed to simulate the load cases according to table 1. The friction coefficient, the number of clamps and the wheel load were varied as well. Two vertical loads were considered in the case of empty ( $Q=50$  kN) and laden vehicle ( $Q=100$  kN). The input data and the main results for the simulated scenarios are shown in table 2.



**Table 2.** Input data and main results of the simulated scenarios

Input data					Main results		
Load case	# Left clamps	# Right clamps	Friction coefficient [-]	Wheel load [kN]	Stopping distance [m]	Acceleration [m/s <sup>2</sup> ]	Rail lift [mm]
1	5	5	0.2	50	5.0	-1.7	160
1	5	5	0.2	100	5.0	-1.7	60
1	5	5	0.1	100	10.0	-0.8	21
1	3	3	0.2	100	9.0	-0.9	28
1	2	3	0.2	100	9.5	-0.9	28
2	2	2	0.2	100	4.5	-0.8	16

Results show that the requirements in terms of stopping distance and maximum deceleration are all satisfied. In the case of five clamps per rail, the resulting braking force is 550 kN per side of the buffer stop and the force that lifts the rail is 180 kN which is equally split at the two ends of triangular structures. The resulting force passing through the strut is 580 kN.

The maximum lift of the rail, i.e. 160 mm, is obtained in the unrealistic case in which load case 1 is combined with a stopping distance of 5 m only and the vertical wheel load is barely  $Q=50$  kN. This deformation value is still compatible with the sleeper's height (common values are 180 and 220 mm), that remain in their position within the ballast, while the maximum stress on the rail is lower than the yield strength of the R260 rail steel (560 MPa). Some results from simulation are shown in figure 8. This confirms that the design is capable to keep both rail deformations and stresses low without the need to stiffen and reinforce the rails.

As maximum forces are exerted in the case with five clamps per rail, the stresses on the buffer stop components are evaluated only for that case and compared with the yield strength of the steel used (355 MPa). For the P10 cast iron used for the braking blocks, their Brinell hardness in the range of 197~255 HB corresponds to a tensile strength of 350 MPa according to 0. As cast iron does not shown relevant plastic deformation this value can be considered as the yield stress.

During the life span of the buffer stop (40 years), the structure will be subjected to a maximum number of 280 load cycles, which is lower than the commonly used minimum value (1000) that requires to consider fatigue. A static stress evaluation is therefore sufficient. Equivalent stresses calculated with the Von-Mises criterion for all the components of the buffer stop are shown in figure 9. A buckling analysis of the strut was performed to check potential stability issues due to the compressive force obtaining a safety factor of about 3.5.

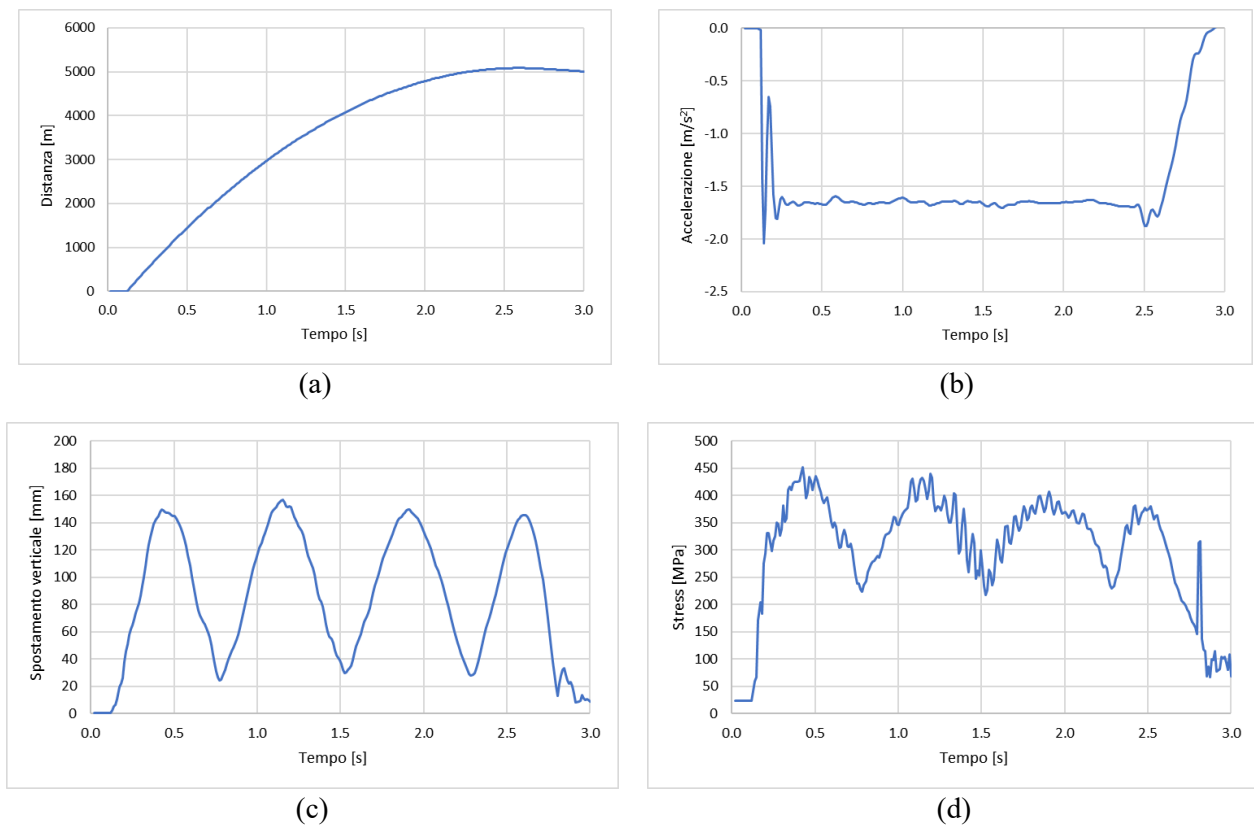


**Figure 8.** Results from the most unfavourable dynamic simulation: stopping distance (a), braking acceleration (b), rail lift (c) and rail stress (d).

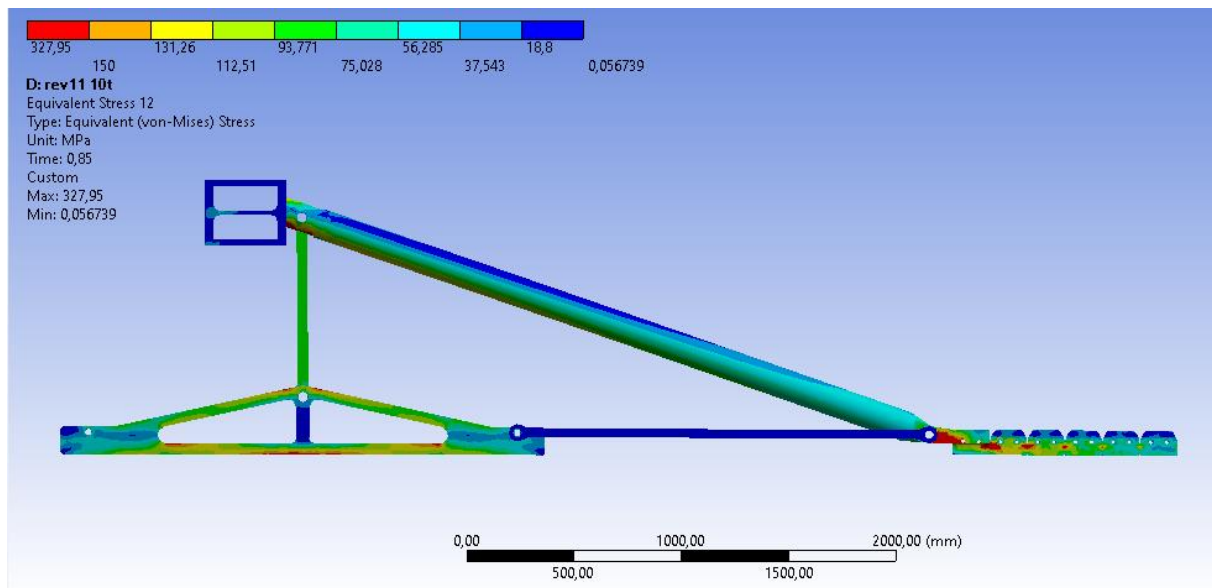


**Figure 9.** Von-Mises stresses as results of the dynamic simulation of the worst case.

## 4. Conclusions

Energy dissipation (friction) buffer stops are widely used at dead end tracks to mitigate the consequences of failed/insufficient braking of moving or theoretically standstill trains. Friction exerted at the interface between clamps and the rail head is used to dissipate the kinetic energy of the moving train hitting the buffer stop. Friction buffers stops are cheaper than hydraulic buffer stops and can absorb a large amount of energy depending on the number of clamps and their preload. Existing friction buffer stops are bulky and made of complex and expensive welded and/or bolted steel profiles. Installation costs are further increased by the need of reinforcing/stiffening the track to reduce the risk of rail failure. Moreover, the dynamic performances of buffer stops are not properly assessed considering the full interaction between the hitting mass, the buffer stop structure, the clamps and the track structure.

In this paper an innovative friction buffer stop was introduced, and the FEM model used to verify its dynamic behaviour was described. The results of the simulation showed that this simple and low-cost structure is suitable to withstand the impact forces resulting from the load cases of the Italian standard, which describes two different configurations. While existing designs need a special track reinforcing system in the case of major impacts, the complete model of the new buffer stop, of the track with the track and of the hitting vehicle shows that any damage is prevented. The simpler design of the clamps led to a more accurate estimation of the braking forces and therefore to a better verification of the dynamic performances of the buffer stop in terms of stopping distances and braking decelerations.

Further modelling improvements could be made considering the impact mass as a set of masses connected by elastic elements instead of a single mass. This could help to validate the behaviour of the buffer stop when the colliding mass is a real train. The peculiar non-linear behaviour of the connections between vehicles, i.e. screw and vehicle buffer, needs specific modelling strategies for an accurate assessment of the longitudinal dynamic of railway vehicles. This topic will be covered in a future paper.

## References

- [1] UIC 544-1. Brakes – Braking power. 2004
- [2] Network Rail. Leaves on the line. <https://www.networkrail.co.uk/running-the-railway/looking-after-the-railway/delays-explained/leaves/> (accessed 19.09.2023)
- [3] White B, Watson M, Lewis R. A year-round analysis of railway station overruns due to low adhesion conditions. *Proceedings of the Institution of Mechanical Engineers, Part F: Journal of Rail and Rapid Transit*. 2023 Apr 1;237(4):458–69.
- [4] Bosso N, Gugliotta A, Magelli M, Oresta IF, Zampieri N. Study of wheel-rail adhesion during braking maneuvers. *Procedia Structural Integrity*. 2019;24:680–91.
- [5] Trummer G, Buckley-Johnstone LE, Voltr P, Meierhofer A, Lewis R, Six K. Wheel-rail creep force model for predicting water induced low adhesion phenomena. *Tribology International*. 2017 May 1;109:409–15.
- [6] Rete Ferroviaria Italiana. Specifica Tecnica di Fornitura – Paraurti ad azione frenante. 2021.
- [7] Israel Railways LTD. Technical specification for manufacture and supply of friction buffer-stops, fixed buffer stops and braking wheel stop sets. 2020.
- [8] UIC 832. Technical specification for the supply of brake-shoes made from phosphoric iron for tractive and trailing stock. 2004
- [9] EN 15551. Railway applications – Railway rolling stock – Buffers. 2017
- [10] EN 16019. Railway applications – Automatic coupler – Performance requirements, specific interface geometry and test method. 2014.  
EN 1561, Founding – Grey cast irons, 2011.